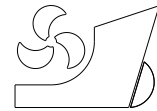


Cheng Zhao
Wei Wang
Panpan Jia
Yonghe Xie



<http://dx.doi.org/10.21278/brod72403>

ISSN 0007-215X
eISSN 1845-5859

OPTIMISATION OF HULL FORM OF OCEAN-GOING TRAWLER

UDC 629.5.015.2:629.5.018.71:629.562.2

Original scientific paper

Summary

This paper proposes a method for optimising the hull form of ocean-going trawlers to decrease resistance and consequently reduce the energy consumption. The entire optimisation process was managed by the integration of computer-aided design and computational fluid dynamics (CFD) in the CAESES software. Resistance was simulated using the CFD solver and STAR-CCM+. The ocean-going trawler was investigated under two main navigation conditions: trawling and design. Under the trawling condition, the main hull of the trawler was modified using the Lackenby method and optimised by NSGA-II algorithm and Sobol + Tsearch algorithm. Under the design condition, the bulbous bow was changed using the free-form deformation method, and the trawler was optimised by NSGA-II. The best hull form is obtained by comparing the ship resistance under various design schemes. Towing experiments were conducted to measure the navigation resistance of trawlers before and after optimisation, thus verifying the reliability of the optimisation results. The results show that the proposed optimisation method can effectively reduce the resistance of trawlers under the two navigation conditions.

Key words: Ocean-going trawler; SBD technique; Lackenby method; FFD method; Towing experiment

1. Introduction

The advancement of hull geometric deformation technology and computational fluid dynamics (CFD) method as well as the application of optimisation technology to ships led to the development of simulation-based design (SBD) technology. This technology, which combines computer-aided design and CFD, considers hydrodynamic performance as the optimisation objective in terms one or more aspects [1]. With given design variables and constraints, the optimisation objective is numerically predicted by the CFD technology; then, the search for the best scheme in the design space is conducted by geometric reconstruction and optimisation techniques.

Many authors have implemented numerous studies on optimising the ship form. Scott et al. (2001) used the CFD tool to compare the calm-water drag of a series of hull forms and define 'optimised' monohull ships for which the total calm-water drag is minimised [2].

Shengzhong et al. (2013) described the fundamental elements of the SBD technique and profoundly analysed crucial components [3].

The SBD technology has enabled the rapid optimisation of ship form. To obtain a hull form with the minimum wave-making resistance, Baoji (2009) proposed an optimisation design method based on the CFD that combines the Rankine source method with nonlinear programming [4]. Mark (2011) used a multi-objective genetic algorithm to optimise the hull form of fishing vessels. To modify the hull shape, optimisation employs three performance indices: resistance, seakeeping, and stability. Consequently, optimal hull offsets and optimal values for principal parameters (length, breadth, and draft) are derived [5]. Soonhung et al. (2012) used parametric modelling to optimise the global shape of an ultra-large container ship and the forebody hull form of an LPG carrier [6]. Bagheri et al. (2014) proposed a computational method to estimate ship seakeeping in regular head waves. In the optimisation process, the genetic algorithm is linked to the computational method to obtain an optimum hull form considering displacement as a design constraint [7]. Baoji et al. (2015) optimised the ship using the minimum total resistance hull form design method based on the potential flow theory of wave-making resistance and considering the effects of tail viscous separation; they finally obtained a ship form with low resistance [8]. Jianwei et al. (2017) modified the hull shape using the shifting and free-form deformation (FFD) methods, predicted the ship resistance by the Neumann–Micell theory, and optimised the ship hull form of a surface combatant model using NSGA-II algorithm [9]. Zhang and DongJoon (2020) employed the Lackenby and FFD methods to modify the hull shape and optimised the catamaran hull shape by considering the wave resistance of the ship in calm water as the optimisation goal [10]. Hayriye (2020) examined the capabilities of Kriging and establish the learning performance according to selected optimization algorithm for multidimensional ship design problem [11]. Le (2021) et al. presented a high-efficiency ship hydrodynamic optimisation tool based on potential flow to optimise hull forms for reducing calm-water resistance and improving vertical motion performance in irregular head waves [12].

Most of the research on ship form optimisation focuses on the hydrodynamic performance of ships under a single navigation condition. Moreover, few scholars analyse and optimise this performance under multiple navigation conditions in the optimisation process. By considering an ocean-going double-deck trawler as an example, this study calculates and examines the hull form optimisation of the trawler under two typical navigation conditions: trawling and design.

The ocean-going trawler is subjected to long working time and characterised by high energy consumption. To fully minimise the resistance and reduce energy consumption, the trawler's hull line and bulbous bow are optimised under trawling and design conditions, respectively. Because of the vessel's navigation resistance, the hull form is optimised by the SBD technology. The hull shape is modified using the Lackenby (1950) and FFD (1986) methods [13][14]. The navigation resistance is calculated by the STAR-CCM+ software, and design schemes are generated by NSGA-II and other algorithms.

2. Numerical Simulation

This research is based on a 32-m ocean-going double-deck trawler; the main information on this vessel is summarised in Table 1. According to the actual use of the vessel, the trawling operation (speed: 4–5 kn) accounts for most of its work. For numerical simulation, the middle values between the beginning (average draft: 3.4 m; trim value: -0.1 m) and end (average draft: 3.44 m; trim value: -0.64 m) of trawling are selected as data under the trawling condition. To optimise ship resistance, the trawler hull line is modified under this condition. Under the design condition, the shape of the bulbous bow is modified based on the optimised

ship form under the trawling condition to achieve less resistance. The specific navigation conditions of the trawler are listed in Table 2. The schematic of the model is shown in Fig. 1.

Table 1 Principal trawler dimension

L_{OA} (m)	L_{PP} (m)	B (m)	D (m)	C_P	X_{CB} (m)
33.2	28	9	5.7	0.682	-0.717

Table 2 Navigation conditions of trawler

Conditions	Speed (kn)	Draft (m)	Trim value (m)	Time proportion (%)
Design condition	10.2	3.5	--	30
Trawling condition	4.5	3.605	-0.37	70

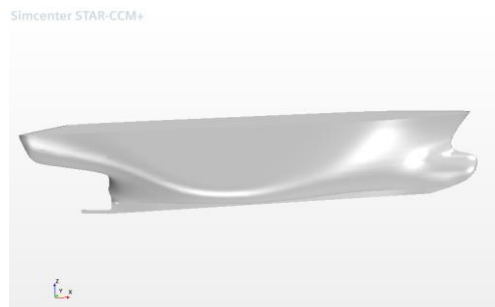


Fig. 1 Side view of model

In this study, resistance was simulated in the STAR-CCM+ software and fed back to the CAESES software by coupling these two programs; ship resistance is calculated using the selected software.

Andrea et al. (2017) used STAR-CCM+ software to calculate the total resistance of a tanker model under different grid density and turbulence model. The numerical simulation results were agreement with the experimental results [15].

In the calculation process, Euler multi-phase flow is employed to model water and air, and the waves obtained by the VOF method are used to represent the interface between water and air. Because the flow around the ship is turbulent, and the Reynolds number is considerable, the realisable K-Epsilon two-layer model is used to describe the influence of turbulence [16].

The calculation domain (Fig. 2) is set as follows: longitudinal, $-4L_{pp} \leq X \leq 2L_{pp}$; transverse, $0 \leq Y \leq 2L_{pp}$; and vertical, $-2L_{pp} \leq Z \leq L_{pp}$.

To mesh the calculation domain and area near the hull surface, trimmed cell mesh and prism layer mesh are used, respectively. The trimmed cells are polyhedral cells; however, they can be typically recognised as hexahedral cells with one or more corners and/or edges cut off. The trimmed mesh has virtually the same filling ratio and accuracy as the structured mesh, but it is easier to generate. By setting the prism layer mesh to generate the boundary layer, precise calculation results for the fluid near the wall can be obtained [14]. The number of grids is 1 209 319; the meshes are shown in Fig. 3.

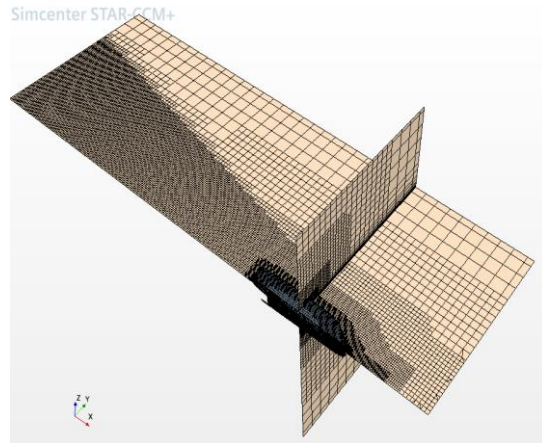
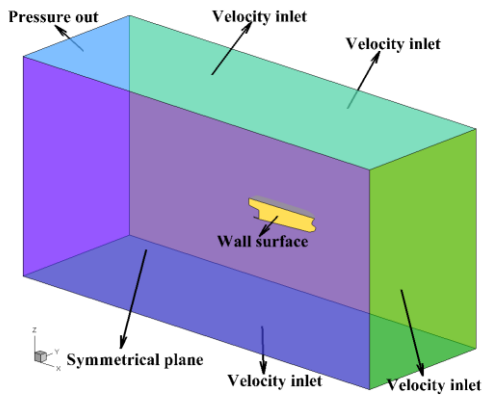


Fig. 2 Computational domain and coordinate system

Fig. 3 Sketch map of mesh generation

3. Hull optimisation

Using the CAESES software, the geometric shape of the ship hull is modified by the Lackenby method [12]. The changes in the centre of buoyancy and displacement are controlled to transform the shape of the main hull. The optimisation design flowchart is shown in Fig. 4.

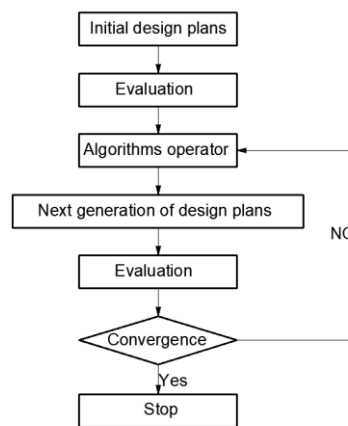


Fig. 4 Optimisation process in CAESES

Under the trawling condition, resistance is calculated, and the hull shape of the trawler is optimised. In the optimisation process, the optimisation objective function is the total resistance of the ship; constraint condition: $-1\% \leq \Delta \leq 1\%$; the control variable: $-1\% \leq \Delta C_p \leq 1\%$ and $-1\% \leq \Delta X_{CB} \leq 1\%$.

The shape transformation diagram of the trawler is shown in Fig. 5.

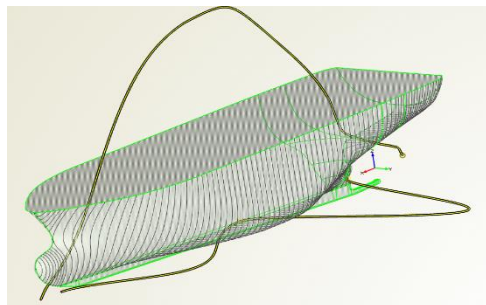


Fig. 5 Surface deformation diagram by Lackenby method

Two optimisation methods are employed.

(1) Using the combination of Sobol and Tsearch algorithms, 60 design calculations are conducted within the range of design variables using the sampling algorithm, Sobol. Based on the preliminary optimisation results, the gradient optimisation algorithm, Tsearch, is applied to optimise 59 schemes [17][18].

(2) NSGA-II is used for optimisation calculations [19] with the population size set to 12, and the number of iterations is 10.

The optimisation results are shown in Figs. 6 and 7.

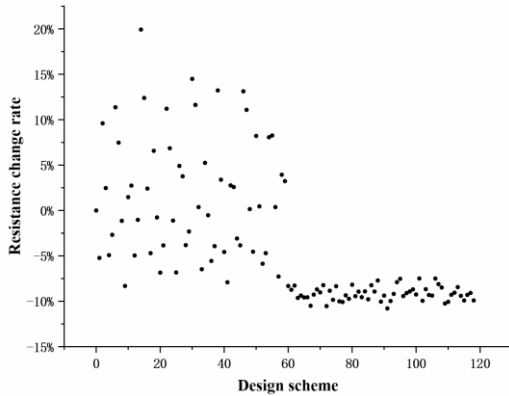


Fig. 6 Results of Sobol + Tsearch algorithm

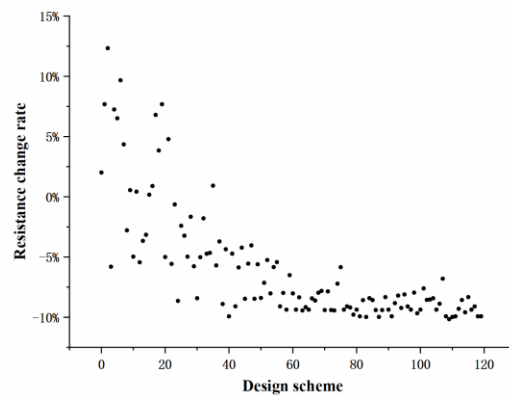


Fig. 7 Results of NSGA-II

The aforementioned figures indicate that the results obtained by the two algorithms are similar. Compared with the original ship form, the resistance of the trawler optimised by Sobol + Tsearch is reduced by 10.8% ($\Delta C_p = -0.9516\%$, $\Delta X_{CB} = 0.9749\%$, and change in $\Delta = -0.944\%$). The resistance after NSGA-II optimisation is reduced by 10.2% ($\Delta C_p = -0.8696\%$, $\Delta X_{CB} = 0.9089\%$, and change in $\Delta = -0.902\%$). The scheme yielding the lowest trawler resistance is selected from a total of 239 optimisation stratagems.

Under the design condition, the resistance of the optimised trawler is reduced by 9.2%.

4. Bulbous bow optimisations

The correct bulbous bow can effectively improve the hydrodynamic characteristics of the ship. Nastia et al. (2021) investigated the influence of three different types of bulbous bow on the resistance of the yacht by means of numerical simulation and towing tank test, the results indicate that the decrease in the total resistance due to bulbous bow can be up to 7% [20].

As illustrated in Fig. 8, the bulbous bow has five main geometric parameters: relative protrusion length, l_b/L_{PP} ; relative flooding depth, h_b/d ; maximum width ratio, b_{max}/B ; bow area ratio, A_{fb}/A_m ; and relative drainage volume ratio, δ/∇ . Yang et al. (2001) found that the maximum width ratio, b_b , is generally 0.26–0.46; the relative protrusion length, l_b , is 0.027–0.04; and the values of relative flooding depth, h_b , are 0.4–0.5 ($Fn < 0.2$) and 0.2–0.4 ($Fn > 0.2$) [21]. Liang et al. (2009) presumed that the bulbous bow was applicable to the speed range $0.25 < Fn < 0.38$. The area ratio of the bulbous bow of ships with a small block coefficient of fishing vessels is usually $f_b = 5\%–15\%$, and the relative length of the bulbous bow is $l_b = 0\%–7.5\%$ [22]. Table 3 summarises the three geometric parameters of the trawler's bulbous bow.

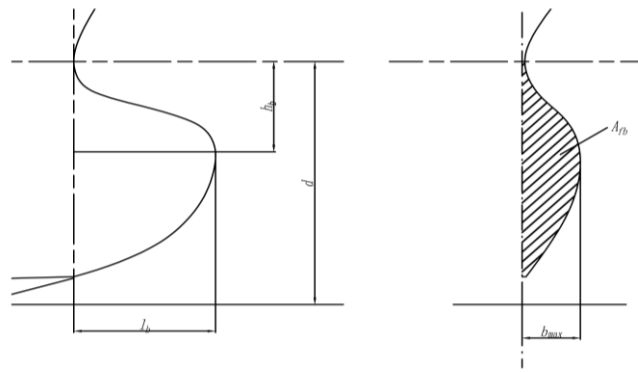


Fig. 8 Geometric parameters of bulbous bow

Table 3 Geometric parameters of bulbous bow of trawler

	Area ratio of bulbous bow	Relative protrusion length	Relative flooding depth
Value	5.7%	6.4%	38.8%

Based on the optimised ship form under the trawling condition, and through the FFD surface deformation function in CAESES, the shape of the bulbous bow is modified, the resistance of trawlers with different bulbous bows is calculated by STAR-CCM+, and the effects of the three geometric parameters (i.e., relative protrusion length, bow area ratio, and relative flooding depth) on the hydrodynamic performance of the trawler under the design condition are studied. Figures 9–11 show how the FFD method is applied to the bulbous bow.

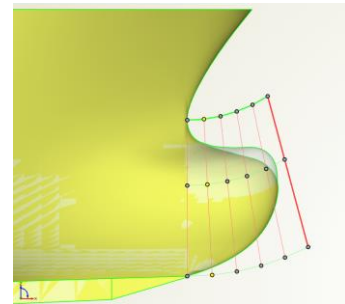
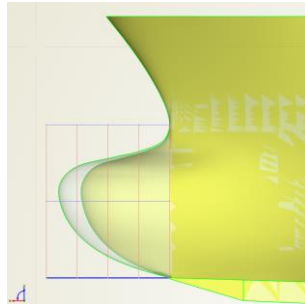
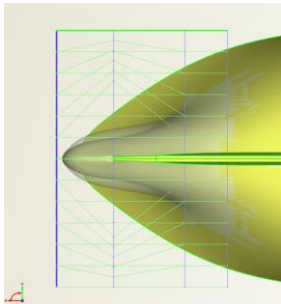


Fig. 9 Variation in bulbous bow area **Fig. 10** Variation in protrusion length **Fig. 11** Variation in flooding depth

4.1 Bulbous bow area ratio

The bulbous bow area ratio is defined as the ratio of the bulbous bow sectional area, A_{fb} , at the stem to the midship sectional area, A_m . The original bulbous bow is used as the mother shape to control the smoothness of the transition section between the bulbous bow and main hull. The resistance calculation is performed for the hull shape with the bulbous bow area ratio ranging from 4.7% to 14.4%; results are shown in Fig. 12.

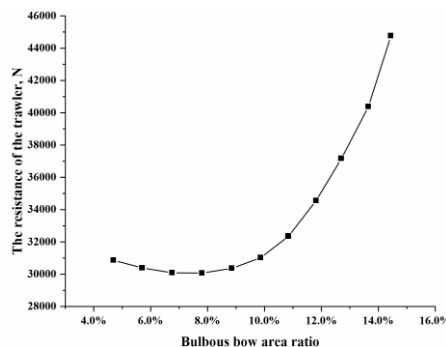


Fig. 12 Resistance under different bulbous bow area ratios

Figure 12 shows that with the increase in the bow area ratio, the trawler resistance first decreases and then increases. When the area ratio is within 4.7%–9.9%, the resistance is small. When the area ratio exceeds 10%, the ship resistance rapidly increases, and the resistance reduction efficiency of the bulbous bow is low.

4.2 Relative protrusion length of bulbous bow

The relative protrusion length of bulbous bow is the ratio of the distance, l_b (from the front end of the bulbous bow to the stem) to L_{PP} . The bow area ratio is set as 7.8%, and the resistance under different relative protrusion lengths is calculated; results are shown in Fig. 13.

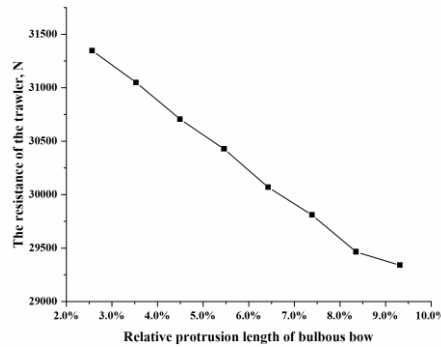


Fig. 13 Resistance under different relative protrusion lengths of bulbous bow

As shown in Fig. 13, the trawler resistance decreases as the relative protrusion length of the bulbous bow increases. Under the condition of satisfying the equipment layout and working conditions of the trawler, the protrusion length of bulbous bow must be increased to the extent possible.

4.3 Relative flooding depth of bulbous bow

The relative flooding depth of bulbous bow is the ratio of the distance, h_b (from the foremost point of the bulbous bow to the calm water surface) to the draft. The relative flooding depth of the bulbous bow is modified by twisting the FFD control box, setting $(X_{stem}, 0, h_b \text{ (origin)})$ as centre, and considering the bow as positive, positive clockwise, and negative anticlockwise directions, various h_b values are obtained from various twisting angles. When the area ratio of the bulbous bow is 7.8%, and the relative protrusion length values of the bulbous bow are 7.4% and 8.4%, the resistance of the trawler with different relative flooding depths is calculated. The results are shown in Figs. 14–15.

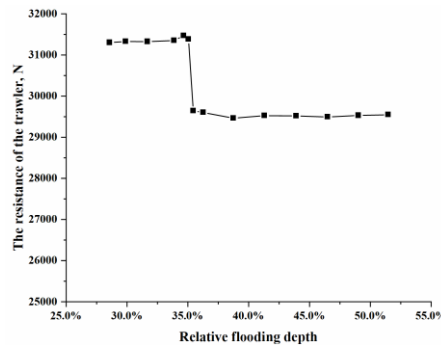


Fig. 14 Resistance at different relative flooding depths when bulbous bow relative protrusion length is 7.4%

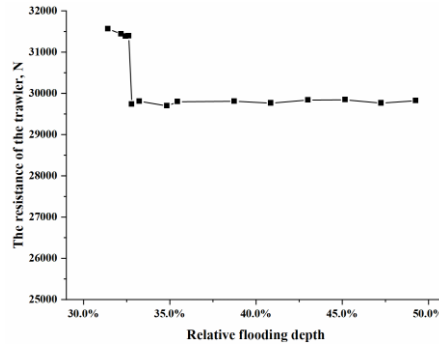


Fig. 15 Resistance at different relative flooding depths when bulbous bow relative protrusion length is 8.4%

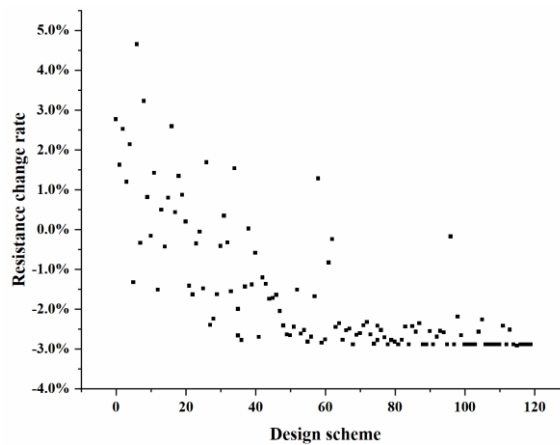
According to Figs. 14 and 15, a critical section for the relative flooding depth of the bulbous bow exists. When the relative flooding depth exceeds the depth in this section, the trawler resistance is generally low, and the resistance reduction performance of the bulbous bow is excellent. If the relative flooding depth is less than the depth in this section, then the resistance of the trawler is generally large. The critical section varies when the protrusion length of the bulbous bow differs.

4.4 Optimisation

Based on the optimised ship form under the trawling condition, the shape of the bulbous bow is modified for further optimisation.

The three variables above are optimised by NSGA-II. The population size to 12 and number of iterations to 10. In the optimisation process, objective function: total trawler resistance; constraint condition: $-1\% \leq \Delta \leq 1\%$; control variable: $-4.7\% \leq$ bulbous bow area ratio $\leq 9.9\%$, $2.6\% \leq$ relative protrusion length $\leq 9.0\%$; and $-15^\circ \leq$ twisting angle $\leq 15^\circ$.

The optimisation results are shown in Fig. 16.



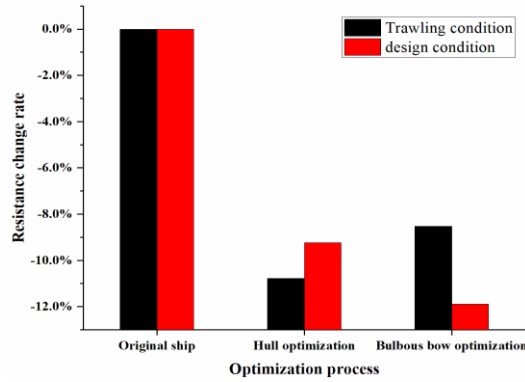


Fig. 17 Resistance variation in different processes

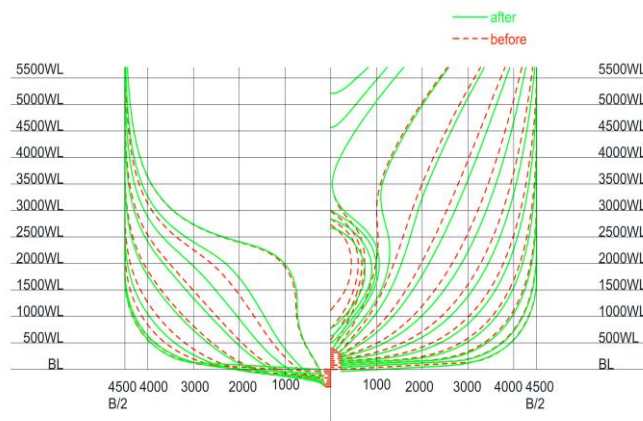


Fig. 18 Comparison of body plan before and after implementing optimization twice

In the optimisation process under constrained displacement, the wetted surface area of the trawler only slightly changed with the hull shape parameters. In the numerical simulation process, the trawler resistance consists of pressure and shear force. The change in resistance mainly emanates from pressure, and the variation in shear is small. Moreover, Figs. 19–20 show the wave pattern comparison of hull form optimisation in different processes under different navigation conditions.

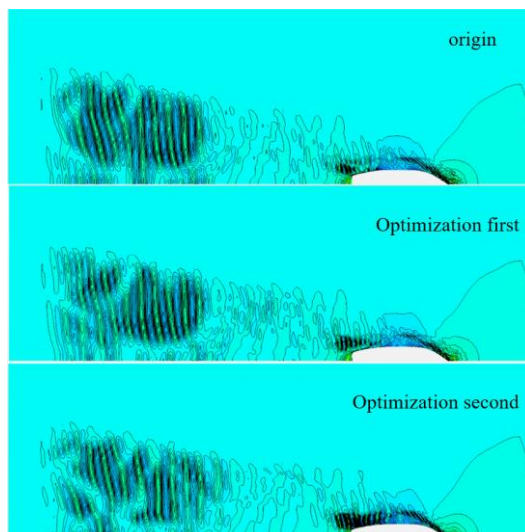


Fig. 19 Wave pattern comparison (under trawling condition)

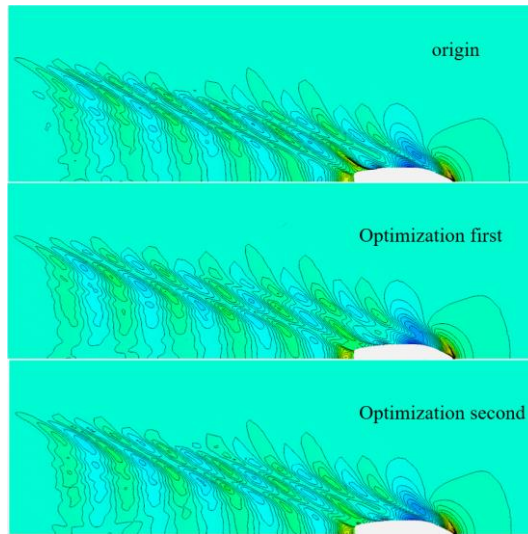


Fig. 20 Wave pattern comparison (design condition)

As shown in Figs. 19 and 20, after the first optimisation, the waves generated by the hull improve, and the trawler resistance is reduced. When the bulbous bow is optimised, the wave generated by the hull increases, thus increasing the trawl resistance. With the improvement in the degree of optimisation under the design condition, the extent of wave improvement around the trawler also increases.

Under the trawling condition, the F_n value of the trawler is 0.139; the trawler is a low-speed ship, and the change in navigation mode is not considered. The trim and surge changes under the design condition are shown in Fig. 21.

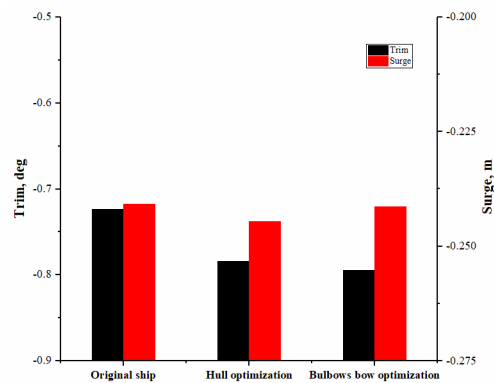


Fig. 21 Trim and surge variations in different processes

5. Experiment

The resistance characteristics of the trawler designed and manufactured in 2012 under the designed draft were predicted using numerical simulation (by Flow-3D software) and physical experiments. In this study, before optimisation, the resistance values at different speeds under the design draft are calculated and compared with the results in the design process to verify the reliability of the numerical simulation. The specific results are shown in Fig. 22.

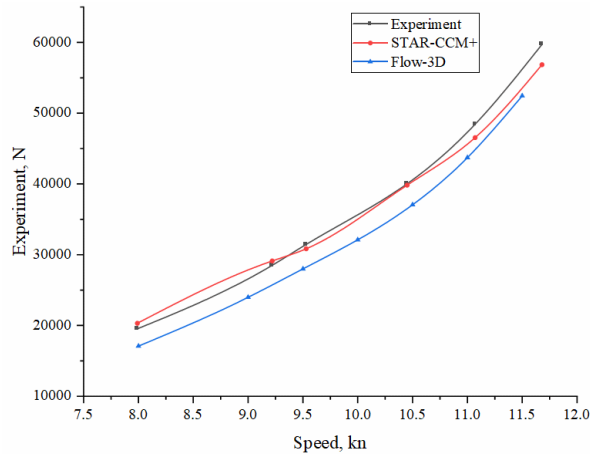


Fig. 22 Comparison between numerical and experimental results

Based on Fig. 22, the change trends of the STAR-CCM+ and Flow-3D results are the same as that of the towing experiment. The difference between the towing experiment and STAR-CCM+ results is less than 5%, and the deviation between the towing experiment and Flow-3D results is less than 15%. The numerical simulation results presented in this paper are found to be reliable [23][24][25].

To further verify the numerical simulation results, additional towing experiments were implemented on the trawler before and after optimisation. The experiment was conducted in the towing tank of the Hydrodynamic Laboratory of Zhejiang Ocean University. The pool size was 130 m × 6 m × 4 m. Wooden models with a scale of 1:10 were used in the experiments. The real ship speed is transformed into that of the ship model speed for the experiment according to the Fn similarity criterion. Two ship models were used in the experiment: the original ship model and the ship model optimised twice. The resistance of the ship model is converted into that of a real ship using a two-dimensional method. The models are shown in Figs. 23 and 24. The diagram of the experimental process is shown in Fig. 25. The specific working conditions are listed in Tables 4 and 5. The comparison of experimental and simulation results is shown in Fig. 26.



Fig. 23 Model of original trawler



Fig. 24 Model of trawler optimised twice



Fig. 25 Towing experiment

Table 4 Principal dimensions of model

L_{OA} (m)	L_{PP} (m)	B (m)	D (m)
3.32	2.8	0.9	0.57

Table 5 Main experimental conditions

Conditions	Fn	Speed (m/s)	Draft (m)	Trim value (m)
Design condition	0.317	1.66	3.5	--
Trawling condition	0.140	0.73	3.605	-0.37

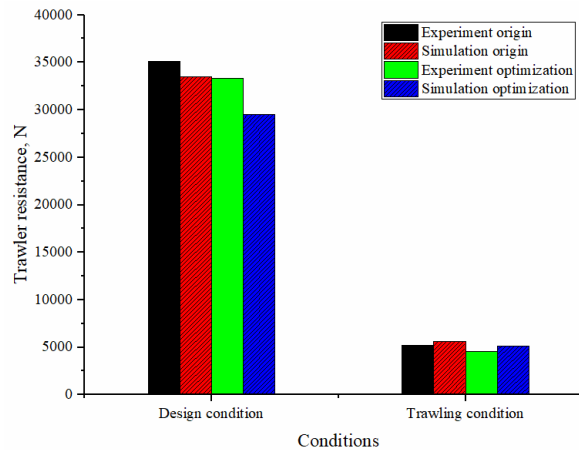


Fig. 26 Experimental and simulation results

Figure 26 indicates that the variations between the numerical simulation and experimental results of the two ship forms before and after optimisation under different working conditions are less than 15%. According to the results of the towing experiment, under the trawling and design conditions, the resistance of the optimised trawler is reduced by 5.2% and 11.7%, respectively.

6. Conclusion

Using the SBD technology, the hull form of the trawler was optimised by coupling the CAESES and STAR-CCM+ software. The hull was optimised using two algorithms, and the forms were generated by the Lackenby method. The bulbous bow of the trawler was optimised using a genetic algorithm, and the forms were generated by the FFD method for various A_b , l_b , and h_b values.

Considering the two commonly used navigation conditions of trawlers, after optimisation, the resistance values of the trawler under the trawling and design conditions were reduced by 8.5% and 11.8%, respectively. Trawler towing experiments were also

implemented before and after optimisation. The experimental results show that the numerical simulation is reliable, and the optimisation loop is feasible and effective. In this study, the main hull and bulbous bow of the trawler are separately optimised; however, these two parameters are found to influence each other. The next work will focus on simultaneously optimising both parameters to determine the best combination.

REFERENCES

- [1] Wang Wenna, Wang Hui. (2017). Research on the cloud platform architecture of ship hydrodynamic structure based on SBD Technology, *Ship Science and Technology*, 39(1A), 4–6, <http://doi.org/10.3404/j.issn.1672-7619.2017.1A.002>
- [2] Scott Percival, Dane Hendrix, Francis Noblesse. (2001). Hydrodynamic optimization of ship hull forms, *Applied Ocean Research*, 23, 337–355, [https://doi.org/10.1016/S0141-1187\(02\)00002-0](https://doi.org/10.1016/S0141-1187(02)00002-0)
- [3] Shengzhong Li, Feng Zhao, Qi-Jun Ni. (2013). Multiobjective optimization for ship hull form design using SBD technique, *Computer Modeling in Engineering and Sciences*, 92, 123–149, <https://doi.org/10.3970/cmcs.2013.092.123>
- [4] Baoji Zhang. (2009). The optimization of the hull form with the minimum wave making resistance based on Rankine source method, *Journal of Hydrodynamics*, 21(2), 277–284, [https://doi.org/10.1016/S1001-6058\(08\)60146-8](https://doi.org/10.1016/S1001-6058(08)60146-8)
- [5] Mark Gammon. (2011). Optimization of fishing vessels using a multi-objective genetic algorithm, *Ocean Engineering*, 38, 1054–1064, <https://doi.org/10.1016/j.oceaneng.2011.03.001>
- [6] Soonhung Han, Yeon-Seung Lee, Young Bok Choi. (2012). Hydrodynamic hull form optimization using parametric models, *Journal of Marine Science and Technology*, 17, 1–17, <https://doi.org/10.1007/s00773-011-0148-8>
- [7] Hassan Bagheri, Hassan Ghassemi, Ali Dehghanian. (2014). Optimizing the seakeeping performance of forms using genetic algorithm, *The International Journal on Marine Navigation and Safety of Sea Transportation*, 8(1), 49–57, <https://doi.org/10.12716/1001.08.01.06>
- [8] Baoji Zhang, Zhu-Xin Zhang. (2015). Research on theoretical optimization and experimental verification of minimum resistance hull form based on Rankine source method, *International Journal of Naval Architecture and Ocean Engineering*, 7, 785–794, <https://doi.org/10.1515/ijnaoe-2015-0055>
- [9] Jianwei Wu, Xiaoyi Liu, Min Zhao, Decheng Wan. (2017). Neumann–Michell theory-based multi-objective optimization of hull form for a naval surface combatant, *Applied Ocean Research*, 63, 129–141, <https://doi.org/10.1016/j.apor.2017.01.007>
- [10] Zhang Yongxing, DongJoon Kim. (2020). Optimization approach for a catamaran hull using CAESES and STAR-CCM+, *Journal of Ocean Engineering and Technology*, 34(4), 272–276, <https://doi.org/10.26748/KSOE.2019.058>
- [11] Hayriye Pehlivan Solak. (2020). Multi-dimensional surrogate based aft form optimization of ships using high fidelity solvers, *Brodogradnja*, 73(1), 85–100, <http://dx.doi.org/10.21278/brod71106>
- [12] Le Zha, Renchuan Zhu, Liang Hong, Shan Huang. (2021). Hull form optimization for reduced calm-water resistance and improved vertical motion performance in irregular head waves, *Ocean Engineering*, 233, 109208, <https://doi.org/10.1016/j.oceaneng.2021.109208>
- [13] Lackenby H. (1950). On the systematic geometrical variation of ship forms. *Trans. INA*92, 289–315.
- [14] Thomas Sederberg, Scott Parry. (1986). Free-form deformation of solid geometric models, *ACM Siggraph*, 151–160, <https://doi.org/10.1145/15886.15903>
- [15] Andrea Farkas, Nastia Degiuli, Ivana Martić. (2017). Numerical simulation of viscous flow around a tanker model, *Brodogradnja*, 68(2), 109–125, <http://dx.doi.org/10.21278/brod68208>
- [16] Simcenter. (2020). USER GUIDE: STAR-CCM+, Version 15.02.
- [17] Stephen Joe, Frances Kuo. (2003). Remark on Algorithm 659: Implementing Sobol's quasirandom sequence generator, *ACM Trans. Math. Softw.*, 29, 49–57. <https://doi.org/10.1145/641876.641879>
- [18] Abdesslem Layeb. (2021). The Tangent Search Algorithm for Solving Optimization Problems. arXiv.
- [19] Kalyanmoy Deb, Amrit Pratap, Sameer Agarwal, et al. (2002). A fast and elitist multi-objective genetic algorithm: NSGA-II, *IEEE Transactions on Evolutionary Computation*, 6(2), 182–197. <https://doi.org/10.1109/4235.996017>

- [20] Nastia Degiuli, Andrea Farkas, Ivana Martić, Ivan Zeman, Valerio Ruggiero, Vedran Vasiljević. (2021). Numerical and experimental assessment of the total resistance of a yacht. *Brodogradnja*, 72(3), 61-80, <http://dx.doi.org/10.21278/brod72305>.
- [21] Yang Youzong, Yang Yi, Cheng Wenyi, Hu Jingtao, Zhang Peixing, Wang Gangyi. (2001). Design and research of ship lines. *Naval Architecture and Ocean Engineering*, 2, 18-23, <https://doi.org/10.3969/j.issn.1005-9962.2001.02.005>.
- [22] Liang Jiansheng, Tan Wenxian. (2009). Comparative experimental research on fishing vessel's bulbous bow model in resistance reduction and energy conservation, *Fisher Modernization*, 36(4), 54-58, <https://doi.org/10.3969/j.issn.1007-9580.2009.04.012>.
- [23] Wang Lijun, Zhang Hao, Xie Yonghe. (2017). Drag performance prediction of fishing trawler considering influence of fishing gear, *Ship Engineering*, 39(3), 8-12, <https://doi.org/10.13788/j.cnki.cbgc.2017.03.008>.
- [24] Zhang Weiying, Dong Zhenpeng, Chen Jing, Mao Xiaoxu, Jin Zhao, Hu Lifan. (2018). Study of resistance optimization for shape of bulbous bow of stern trawler based on FLUENT, *Journal of Dalian University of Technology*, 58(2), 124-132, [https://doi.org/1000-8608\(2018\)02-0124-09](https://doi.org/1000-8608(2018)02-0124-09).
- [25] Li Na, Liang Jiansheng. (2018). Analysis of resistance characteristics of 33.2 m ocean-going double deck trawler, *Fishery Modernization*, 45(6), 74-80, <https://doi.org/10.3969/j.issn.1007-9580.2018.06.012>

Submitted: 13.09.2021. Cheng Zhao, S19082400004@zjou.edu.cn
School of Naval Architecture and Maritime, Zhejiang Ocean University

Accepted: 15.11.2021. Corresponding author: Wei Wang, wangwei1981@zjou.edu.cn
1.School of Naval Architecture and Maritime, Zhejiang Ocean University
2.School of Naval Architecture Ocean and Civil Engineering, Shanghai Jiaotong University
3.Marine Design and Research Institute of China

Panpan Jia, 296167636@qq.com
School of Naval Architecture and Maritime, Zhejiang Ocean University

Yonghe Xie, xieyh@zjou.edu.cn
School of Naval Architecture and Maritime, Zhejiang Ocean University